

Neutrino Physics at MiniBooNE

G. P. Zeller

Columbia University Department of Physics
538 W. 120th St., New York, NY 10027, USA
for the MiniBooNE Collaboration

As its primary design goal, the MiniBooNE experiment at Fermilab searches for $\nu_\mu \rightarrow \nu_e$ oscillations in order to confirm or refute the high Δm^2 oscillations reported by the LSND collaboration [1]. In addition to preparing for these much anticipated oscillation results, the experiment is also collecting large samples of low energy neutrino interactions that are proving to be quite valuable. These data sets include ν_μ charged current quasi-elastic, neutral current π^0 , and charged current π^+ interactions in mineral oil.

1. THE ROLE OF MiniBooNE

Many experiments have now provided compelling evidence that neutrinos have mass and can mix [2, 3]. Both the solar and atmospheric indications of neutrino oscillations have been corroborated by multiple experiments and detection techniques. The solar neutrino experiments point to a favored mass-squared splitting of $\Delta m_{solar}^2 \cong 7 \times 10^{-5}$ eV². The atmospheric results indicate a $\Delta m_{atm}^2 \cong 2.5 \times 10^{-3}$ eV². At even higher Δm^2 , there remains unconfirmed evidence for neutrino oscillations obtained by a single accelerator-based experiment, LSND [1]. The LSND evidence for $\bar{\nu}_\mu \rightarrow \bar{\nu}_e$ transitions favor $\Delta m_{LSND}^2 \cong 1$ eV². The separate solar, atmospheric, and LSND values of neutrino mass-squared differences (Figure 1) are inconsistent with only three active neutrino species because

$$\Delta m_{LSND}^2 \neq \Delta m_{solar}^2 + \Delta m_{atm}^2. \quad (1)$$

The violation of this simple constraint demands a drastic solution. For instance, one or more of the experiments might in fact *not* have observed neutrino oscillations, but something else. Or perhaps there exist one or more sterile (non-weakly-interacting) neutrinos which would allow at least three distinct mass-squared differences. Although other possible explanations for the inconsistent scales have included CPT violation and neutrino production from lepton flavor violating decays (in the case of the LSND observation), these particular solutions have become less viable recently [5, 6]. Without regard to the theoretical challenges, experimental verification or refutation of the oscillations reported by LSND is crucial. MiniBooNE's prime function is to serve this role.

2. THE MiniBooNE NEUTRINO BEAM

The MiniBooNE neutrino beamline was specifically optimized for the direct search for LSND-like oscillations, but is also particularly well-suited for investigations of low energy neutrino interactions. Production of our neutrino beam starts with 8 GeV protons provided by the Fermilab Booster, one of the accelerators in the Fermilab chain. These protons interact in a 71 cm long beryllium target enclosed inside a magnetic horn. This horn serves to focus secondary charged particles produced by the primary protons' interactions. These secondary particles, mostly pions and kaons, decay in a 50 meter long decay region. The result is a flux of neutrinos arriving at the MiniBooNE detector which is $\sim 99.5\%$ pure ν_μ along with a small contamination of ν_e 's. The expected energy distribution of both muon and electron neutrinos at the detector is shown in Figure 2. The mean energy of ν_μ 's at MiniBooNE is approximately 700 MeV.

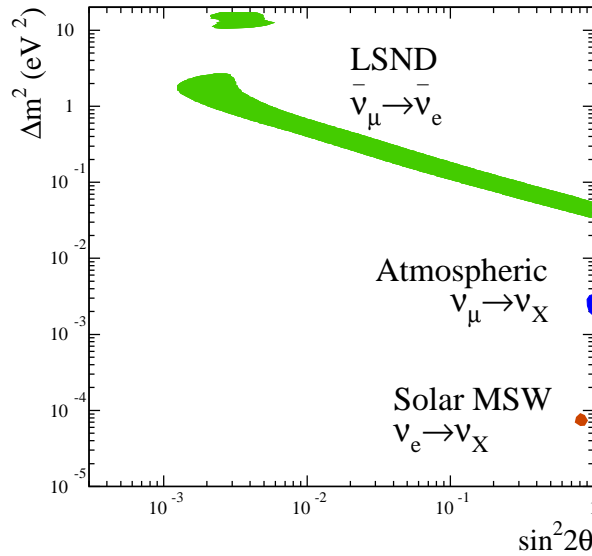


Figure 1: Current status of positive neutrino oscillation signals. Shown are the allowed 90% CL regions in $\sin^2 2\theta$ - Δm^2 space for solar, atmospheric, and LSND neutrino oscillations.

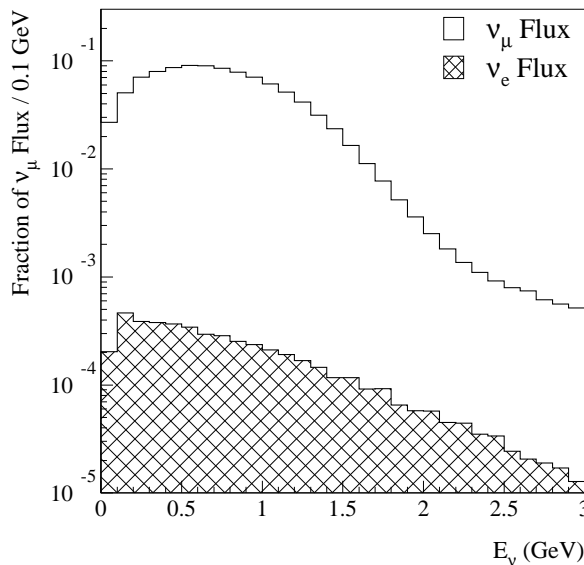


Figure 2: Preliminary expected ν_μ and ν_e energy distributions at the MiniBooNE detector.

3. THE MiniBooNE DETECTOR

The MiniBooNE detector sits 541 meters downstream of the primary proton target. It is a 12 meter diameter spherical tank filled with 800 tons of un-doped mineral oil (CH_2). The inner region of the tank is viewed by 1240 inward-facing photomultiplier tubes (PMTs) providing 10% photocathode coverage of the interior surface. An optical barrier mounted 35 cm from the outer tank wall separates this inner fiducial volume from an outer veto region. The outer region is lined with 240 pair-mounted PMTs and serves as a veto for charged particles both entering or leaving the tank.

Neutrino interactions reveal themselves by the charged particles they produce in the MiniBooNE tank. As they

pass through the mineral oil, these charged particles produce both prompt Čerenkov radiation as well as some amount of delayed, isotropic scintillation light. Each type of final state particle offers its own distinct signature of light in the tank. Electrons are identified by their fuzzy ring shape, characteristic of an electromagnetic shower. Muons have a ring profile with a well-defined, sharp outer edge, characteristic of a penetrating track. Neutral pions are another important and distinct class of particles that are produced in the tank. The $\pi^0 \rightarrow \gamma\gamma$ decay produces twin electromagnetic showers and hence two fuzzy Čerenkov rings, each of which is very similar to an electron ring. Distinguishing these three event classes is important not only for the $\nu_\mu \rightarrow \nu_e$ oscillation search, but also for isolating the various MiniBooNE neutrino event samples. Overall, the particle identification techniques used by MiniBooNE are similar to those employed by other experiments using Čerenkov-based detectors [4].

Along with ring topology, identification of the delayed Michel electron from muon decays also provides an additional form of muon identification. For example, NC π^0 candidates can be initially selected with the requirement that there are no Michel electrons in the event. Requiring two Michel electrons is particularly useful in identifying CC π^+ interactions at MiniBooNE. These event samples are discussed in more detail in the next section.

4. NEUTRINO EVENT SAMPLES AT MiniBooNE

The recent development of intense, accelerator-based neutrino sources has made possible the further exploration of low energy neutrino interactions. This low energy region is particularly interesting both for its richness and complexity (Figure 3).

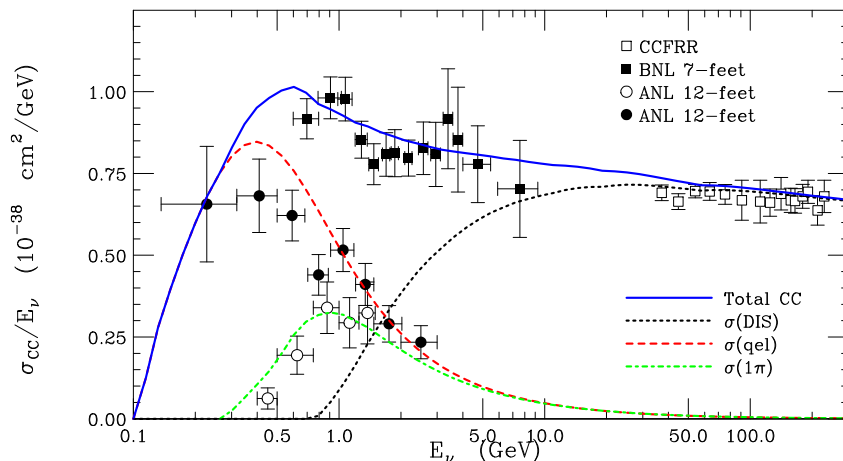


Figure 3: *CC neutrino cross sections as a function of energy. Shown are the contributions from quasi-elastic (QE), single pion (1π), and deep inelastic scattering (DIS) processes. Figure is from [7].*

At energies below a few GeV, neutrino interactions come from a variety of sources. They are predominantly quasi-elastic (QE) and single pion production processes, though deep inelastic scattering (DIS) interactions also begin to contribute. Present day atmospheric and accelerator-based neutrino oscillation experiments primarily operate in this energy region where they rely on current knowledge of the contributing neutrino cross sections. Historically, cross sections in this regime have not been nearly as well measured as DIS reactions which fully dominate at higher neutrino energies. Our current knowledge comes mainly from bubble chamber, spark chamber, and emulsion experiments which collected their data decades ago. These measurements typically suffered from poor statistics and large neutrino flux uncertainties; nonetheless, they offer an important and necessary constraint on Monte Carlo models in present use. The situation is quickly changing with the emergence of new, high statistics neutrino event samples from both the K2K near detector and MiniBooNE.

Table I reports the relative population of events expected at MiniBooNE. Given the incoming neutrino energy spectrum, MiniBooNE enjoys low levels of multi-pion and DIS scattering interactions, and is dominated by elastic

and single pion production. In order to preserve objectivity in the $\nu_\mu \rightarrow \nu_e$ search, MiniBooNE is deliberately “blind-folded” to any possible oscillation signal. Despite this fact, we have access to over 85% of our total collected data. This includes large samples of CC quasi-elastic, NC π^0 , and CC $1\pi^+$ events, which will be discussed in the following three sections. These samples are already yielding important new insight into low energy neutrino phenomena.

Table I: *Expected flux-averaged event fractions for various ν_μ processes at MiniBooNE (no selection cuts). The dominant interactions are quasi-elastic, elastic, and resonant single π production.*

Reaction	Fraction of Total Events
CC QE, $\nu_\mu n \rightarrow \mu^- p$	40%
CC $1\pi^+$, $\nu_\mu N \rightarrow \mu^- N \pi^+$	25%
NC EL, $\nu_\mu N \rightarrow \nu_\mu N$	16%
NC $1\pi^0$, $\nu_\mu N \rightarrow \nu_\mu N \pi^0$	8%
CC $1\pi^0$, $\nu_\mu n \rightarrow \mu^- p \pi^0$	4%
CC (NC) 2π , $\nu_\mu N \rightarrow \mu^- (\nu_\mu) N \pi \pi$	3%
NC $1\pi^\pm$, $\nu_\mu N \rightarrow \nu_\mu N \pi^\pm$	3%
CC (NC) DIS, $\nu_\mu N \rightarrow \mu^- (\nu_\mu) X$	1%

4.1. CC Quasi-Elastic Scattering ($\nu_\mu n \rightarrow \mu^- p$)

The study of ν_μ quasi-elastic scattering is important for several reasons. First, precise knowledge of ν_μ QE cross sections is necessary to predict the signal rates in oscillation searches. Measurement of ν_μ QE interactions provides a necessary constraint to $\nu_\mu \rightarrow \nu_e$ appearance searches because the ν_e QE process has a similar cross section and event kinematics. Because they are charged current interactions, such events also enable reconstruction of the incoming neutrino energy with good resolution. Finally, ν_μ QE samples can additionally be used to search for $\nu_\mu \rightarrow \nu_s$ oscillations with only a single detector through observation of distortions in their expected energy distributions.

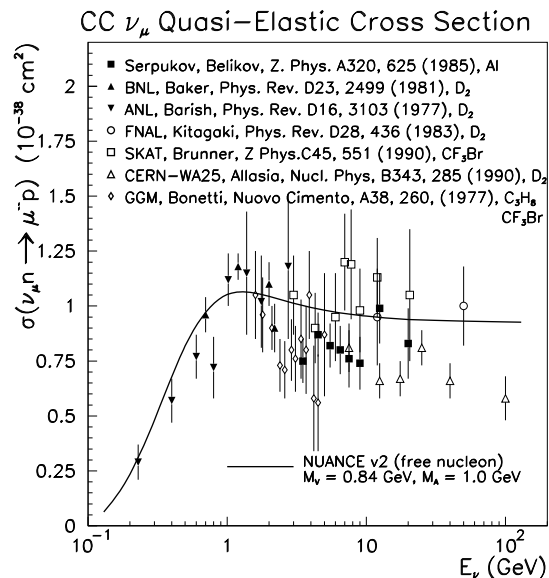


Figure 4: *Existing QE cross section measurements as a function of neutrino energy. Also shown for comparison is the free nucleon QE cross section prediction from the NUANCE Monte Carlo [11].*

Figure 4 provides a collection of the existing QE cross section data that is used to verify the predictions from low energy neutrino Monte Carlo generators in present use. These measurements were made decades ago on a variety

of targets. The highest statistics of any given sample was ~ 2500 events. Much larger data samples from both the MiniBooNE [8] and K2K [9] experiments will provide more stringent constraints on QE scattering at low energy. More importantly, these measurements are being made on nuclear targets (^{12}C , ^{16}O) in a region where heavy target data is currently completely lacking ($E_\nu < \sim 2$ GeV). Additional measurements, based on a sample of approximately 8,000 QE events on carbon in the 3 – 100 GeV energy range, are also expected soon from the NOMAD experiment [10].

Charged current quasi-elastic events are the most copious interactions at MiniBooNE (Table I). Such processes should also be the simplest to study as they are governed by two body scattering kinematics. Clean QE interactions at MiniBooNE are identified by requiring a single Čerenkov ring consistent with expectations for a muon passing through the detector. This requirement, along with fiducial volume and veto cuts, yields a sample that is $\sim 80\%$ pure ν_μ QE [8]. The dominant background arises from CC π^+ interactions in which the final state π^+ is either absorbed in a carbon nucleus or falls below Čerenkov threshold. To reduce the uncertainty from this source of background, the rate of π^+ production in carbon at low energy can be constrained using additional MiniBooNE data (Section 4.3).

MiniBooNE has currently collected roughly 60,000 ν_μ QE events, a factor of five more data than all previous published measurements combined. We expect about an order of magnitude more events in our full data set. Figure 5 compares the distributions of neutrino energy and 4-momentum transfer (Q^2) for our current QE sample. The Monte Carlo expectation includes our present systematics which are expected to improve. While the Monte Carlo prediction agrees well with the data, the difference in the first Q^2 bin has sparked much interest recently as it may point to a deficiency in the nuclear models employed by current low energy neutrino oscillation experiments. This is still under investigation.

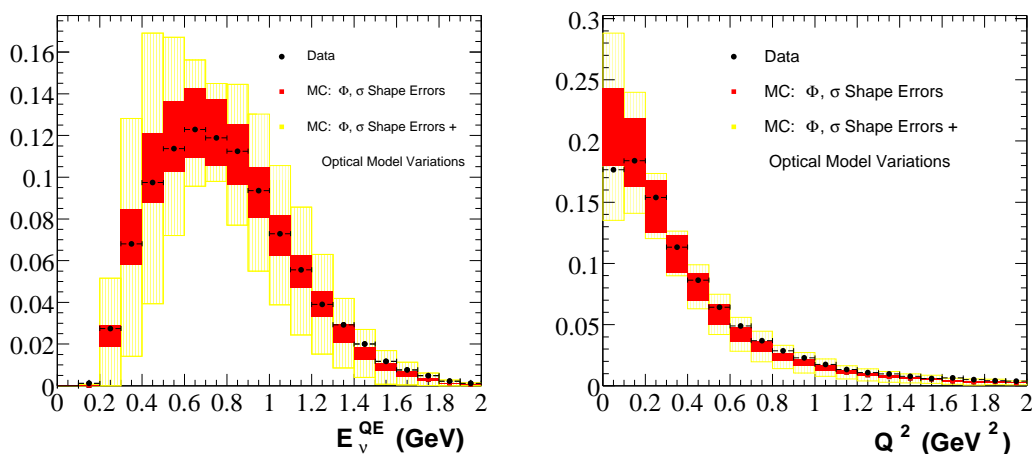


Figure 5: Preliminary distributions of reconstructed E_ν^{QE} and Q^2 for MiniBooNE ν_μ events passing QE selection cuts. The red error bands bracketing the Monte Carlo expectation include our current flux and cross section systematics, while the yellow band indicates variations in our oil optical model. The data and Monte Carlo distributions in both cases are normalized to unit area.

4.2. NC π^0 Production ($\nu_\mu N \rightarrow \nu_\mu N \pi^0$)

Understanding both the rate and kinematics of NC π^0 production is particularly important for $\nu_\mu \rightarrow \nu_e$ oscillation searches because such interactions can mimic an oscillation signal. If the photons from the π^0 decay are either highly asymmetric in energy or have a small opening angle (*i.e.*, produce overlapping Čerenkov rings), the event could look like an electron event. In addition, further study of π^0 production can offer insight into the production mechanism for such events; NC π^0 samples can have contributions from both resonant and coherent production processes, each of which has a distinctive rate and final state kinematics.

The dominant means of single pion production at low energy results from the excitation of baryon resonances which decay to a nucleon-pion final state. At MiniBooNE energies, the primary contribution comes from Δ production. A much smaller fraction of single pions are produced coherently, where the neutrino scatters from the entire

nucleus, transferring negligible energy to the target. The result is a distinctly forward-scattered pion compared to resonant processes. Figure 6 shows the meager status of existing resonant and coherent NC π^0 absolute cross section measurements.

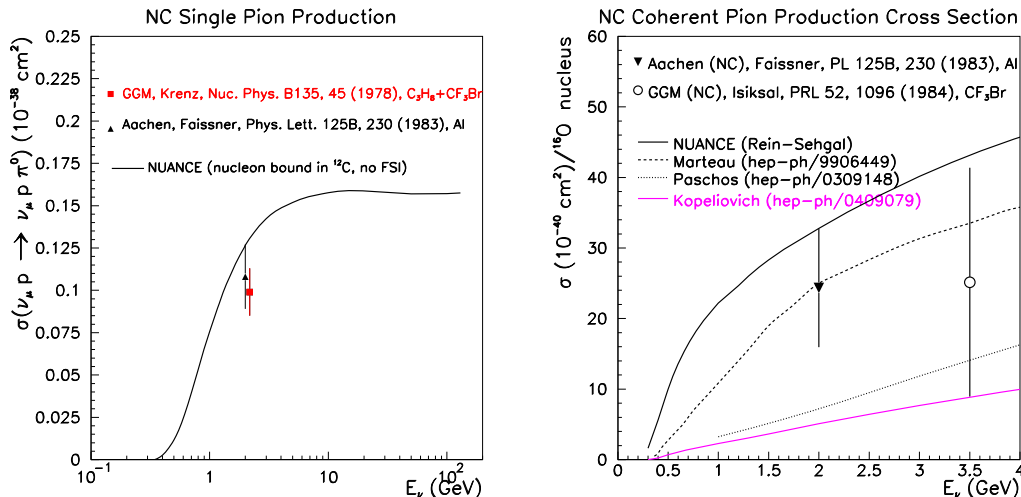


Figure 6: Resonant (left) and coherent (right) NC π^0 cross section measurements at low energy. The NUANCE [11] curve, as plotted, does not include the effects of π^0 absorption in the target which would further reduce the predicted cross section. Also shown in the coherent case are the predictions from several more recent calculations [12].

No published measurements below 2 GeV exist for either process. In the case of resonant NC π^0 production, there are two reported measurements, one from a recent re-analysis of Gargamelle bubble chamber data [13] and the other from a footnote in an early spark chamber paper [14]. Data on coherent π^0 production are more copious, especially at higher energies, but at low energy there are only two reported measurements. As a result, theoretical predictions for coherent rates at low energy vary widely. Current models range up to an order of magnitude in their predictions: a situation which MiniBooNE can certainly help to resolve.

MiniBooNE reconstructs NC π^0 candidate events with a generic two-ring fitting algorithm to determine the direction and energy of each of the rings produced in the $\pi^0 \rightarrow \gamma\gamma$ decay. From this, the resultant decay kinematics can be calculated. Figure 7 displays the reconstructed invariant π^0 mass and π^0 angular distributions from an early MiniBooNE sample containing approximately 13,000 events. Approximately 7,200 are identified as true NC π^0 resonant or coherent signal events.

In both cases, the model cleanly reproduces the details of the π^0 decays. In addition, the π^0 angular distribution can reveal the proportion of π^0 production from resonant versus coherent processes (coherent π^0 production is expected to be much more forward peaked). Although it is too soon to draw any strong conclusions, the MiniBooNE data may in fact suggest a lower coherent π^0 cross section than the most popular model prediction [11].

4.3. CC π^+ Production ($\nu_\mu N \rightarrow \mu^- N \pi^+$)

Charged current π^+ samples can also provide an important and rich field of study. First, such interactions comprise the dominant background to QE samples, occurring at roughly half the rate of QE processes at MiniBooNE energies. Second, they can provide further information on Δ resonance production on nuclear targets. For example, despite having a small branching fraction, radiative Δ decays ($\Delta \rightarrow N\gamma$) can pose a non-negligible background for ν_e appearance searches. Measuring the rate of CC single π^+ interactions at MiniBooNE would help supply an additional constraint on Δ production on carbon. In fact, this would be the first such measurement of single pion production at these energies (Figure 8).

Third, as in the case of NC π^0 production, CC π^+ processes can be produced both resonantly and coherently; thus, studying the muon angular distribution in such events can also shed light on coherent single pion production cross

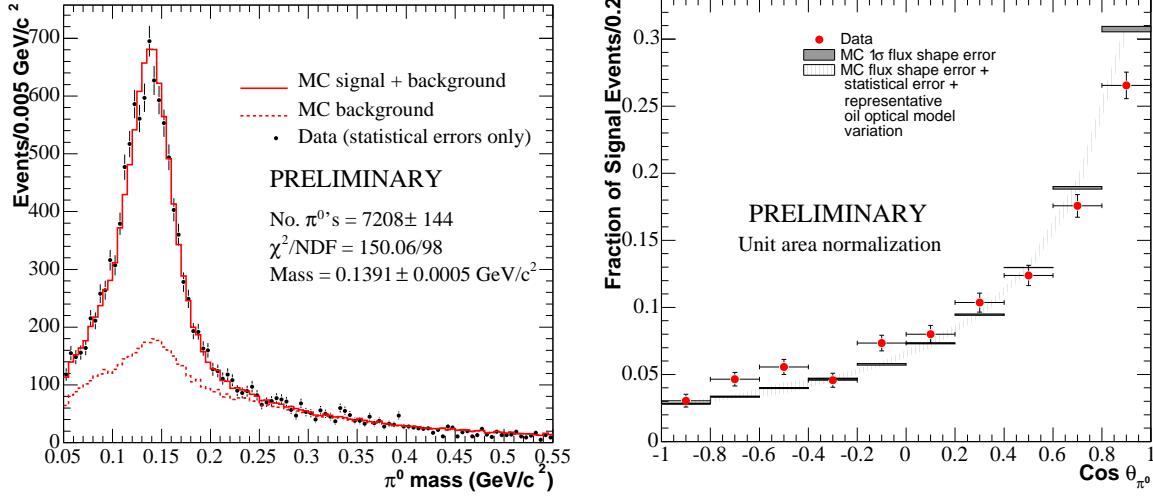


Figure 7: Reconstructed invariant mass (left panel) and pion angular distributions (right panel) for MiniBooNE NC π^0 candidate events. The invariant mass plot includes statistical errors only. In this case, the fitted shapes are Monte Carlo-based parameterizations of the contribution from signal events (solid) as well as non-resonant/non-coherent backgrounds (dashed). The backgrounds may include a π^0 in the final state. The angular distribution is the π^0 yield in $\cos \theta_{\pi}$ bins extracted from a fit to the invariant mass distribution. Data and Monte Carlo are normalized to unit area.

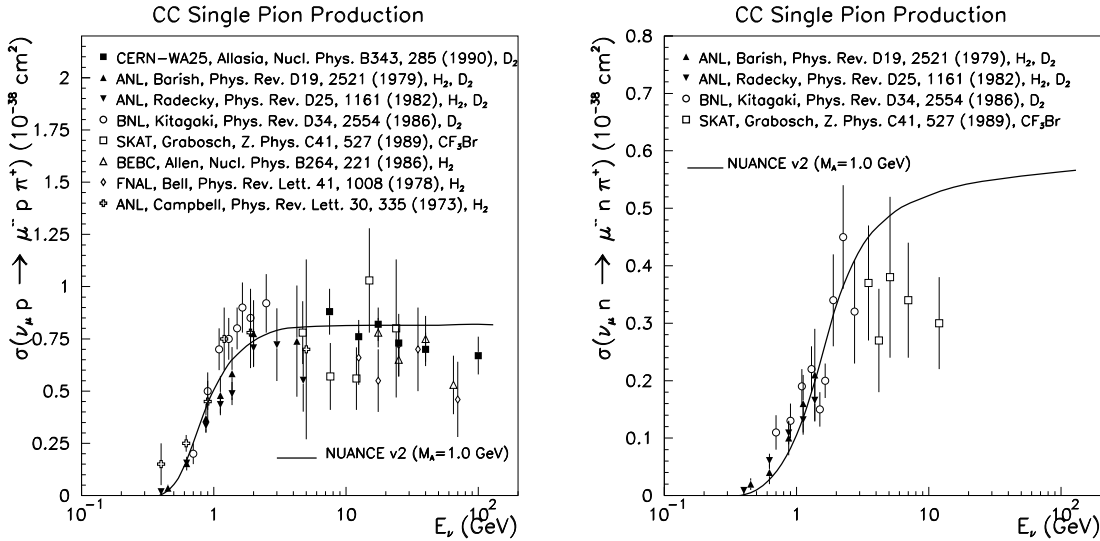


Figure 8: Previous measurements of resonant CC 1π cross sections for $\nu_{\mu} p \rightarrow \mu^{-} p \pi^{+}$ (left panel) and $\nu_{\mu} n \rightarrow \mu^{-} n \pi^{+}$ (right panel). There is no data on heavy targets below $\sim 3 \text{ GeV}$. Also shown is the prediction from NUANCE [11].

sections at low energy. Finally, because of their large expected rate of production, CC π^{+} data samples can also provide a high statistics ν_e CC π^{+} oscillation search to complement the main QE-based ν_e appearance channel.

MiniBooNE isolates CC π^{+} interactions by simply demanding two decay electrons, one each from the pion and primary muon decays. Applying this selection criterion, in addition to fiducial volume and veto cuts, results in a high statistics sample of $\sim 36,000$ events that is 85% pure CC π^{+} [16]. This sample is already an order of magnitude more data than all previous measurements combined. Further results on this sample are forthcoming [16].

5. CONCLUSIONS

In addition to the much anticipated $\nu_\mu \rightarrow \nu_e$ oscillation results, MiniBooNE is poised to make significant advancements to the understanding of low energy neutrino interactions on nuclear targets. The experiment continues to accumulate statistics rapidly. We are also further refining our analyses on CC QE, CC π^+ , and NC π^0 events, samples which are already providing important feedback on how well current Monte Carlo cross section predictions are performing. MiniBooNE also hopes to complement these studies with additional antineutrino running in the near future [17]. Such antineutrino measurements would be the first in this energy range, and are imperative for future precision experiments searching for CP-violation in the neutrino sector.

6. Acknowledgements

The author would specifically like to thank J. Monroe, J. L. Raaf, and M. O. Wascko for their input to this presentation. MiniBooNE gratefully acknowledges the support it receives from the Department of Energy and the National Science Foundation. The presenter of this paper was supported by NSF grant PHY-98-13383.

References

- [1] A. Aguilar *et al.* (LSND collaboration), Phys. Rev. **D64**, 112007 (2001).
- [2] B. Kayser, these proceedings.
- [3] G. Gratta, these proceedings.
- [4] D. Casper, these proceedings.
- [5] J. R. Musser *et al.* (TWIST collaboration), submitted to Phys. Rev. Lett., *hep-ex/0409063*.
- [6] M. C. Gonzalez-Garcia, Phys. Rev. **D68**, 053007 (2003), *hep-ph/0306226*.
- [7] P. Lipari, Nucl. Phys. Proc. Suppl. **112**, 274 (2002).
- [8] J. Monroe (MiniBooNE collaboration), Nucl. Phys. Proc. Suppl. **139**, 59 (2005), *hep-ex/0408019*.
- [9] R. Gran (K2K collaboration), Nucl. Phys. Proc. Suppl. **139**, 54 (2005).
- [10] R. Petti (NOMAD collaboration), to appear in the proceedings of the 32nd International Conference on High Energy Physics (ICHEP04), *hep-ex/0411032*.
- [11] D. Casper, Nucl. Phys. Proc. Suppl. **112**, 161, (2002), *hep-ph/0208030*.
- [12] J. Marteau *et al.*, to be published in the proceedings of the 34th Recontres de Moriond: Electroweak Interactions and Unified Theories, *hep-ph/9906449*; E. A. Paschos *et al.*, *hep-ph/0309148*; B. Z. Kopeliovich, Nucl. Proc. Suppl. **139**, 219 (2005), *hep-ph/0409079*.
- [13] E. A. Hawker (MiniBooNE collaboration), to appear in the proceedings of the 2nd International Workshop on Neutrino-Nucleus Interactions in the Few GeV Region (NuInt02).
- [14] H. Faissner *et al.*, Phys. Lett. **125B**, 230 (1983).
- [15] J. L. Raaf (MiniBooNE collaboration), Nucl. Phys. Proc. Suppl. **139**, 47 (2005), *hep-ex/0408015*.
- [16] M. O. Wascko (MiniBooNE collaboration), to appear in the proceedings of the Annual Meeting of the Division of Particles and Fields (DPF04) conference, *hep-ex/0412008*.
- [17] A. A. Aguilar-Arevalo (MiniBooNE collaboration), MiniBooNE letter of intent, November 2004, <http://www-boone.fnal.gov/publicpages/news.html>.